DOI: 10.1002/chem.200401252

Synthesis and Properties of New Tetrazines Substituted by Heteroatoms: Towards the World's Smallest Organic Fluorophores

Pierre Audebert,* Fabien Miomandre, Gilles Clavier, Marie-Claude Vernières, Sophie Badré, and Rachel Méallet-Renault[a]

Abstract: New tetrazines substituted by heteroatoms have been synthesized and their electrochemical and photochemical properties investigated. All compounds are reversibly electroactive with standard potentials shifting cathodically according to the donor character of the substituent. The tetrazine derivatives are also fluorescent with maximum emission wavelengths in the range 550–575 nm. Some of them show very long fluorescence lifetimes (several tens of ns) and remain fluorescent in the solid state without major changes in the spectral features. The fluorescence of one of the derivatives can be efficiently quenched by the presence of electron-rich compounds such as triphenylamines, phenol or anisole, which make them very promising compounds for sensor applications.

Keywords: electrochemistry · fluorescence · quenching · tetrazines

Introduction

The search for new compounds, which gather optical and electrochemical properties is still very active, given their huge potential in sensors building.[1–4] The fluorescence and reversible electroactivity are particularly interesting properties in this respect, because fluorescent and/or electroactive molecules may be quenched within a given time scale and therefore lead to sensing components according to the quenching agent. The tetrazine family appears a very promising and fascinating class of compound for this purpose. They are highly colored and reversibly electroactive heterocycles, displaying the following special properties:

- They have a very high electron affinity, which make them reducible at high to very high potentials (actually they are the electron poorest C–N heterocycles)[5];
- they have a low lying π* orbital resulting in an n–π* transition in the visible light range.[6–10]

We have already published the synthesis and the electrochemical properties of several bisaryltetrazines,[11] as well as their ability to form new conjugated electroactive polymers.[12]

We, and others,[13] found that some tetrazines had fluorescence properties. In addition, all these compounds which are fluorescent in solution are also fluorescent in the crystalline state; this behavior place them certainly among the smallest crystalline organic fluorophores in the visible range ever prepared, and therefore makes them especially attractive for potential applications as sensors.

In this article we report the synthesis of chloromethoxy-*s*-tetrazine (**2**), dimethoxy-*s*-tetrazine (**3**), the novel chloronaphthoxy-*s*-tetrazine (**4**) and a new bridged tetrazine 1,4-bis(chloro-*s*-tetrazinyloxo)butane (**5**). We also report their electrochemical and fluorescence properties, including the lifetimes of the excited states in solution and solid state, and

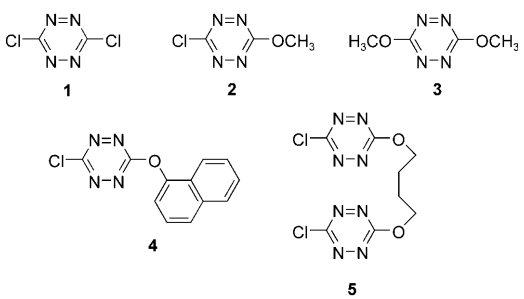

1 2 3 4 5

[a] Prof. P. Audebert, F. Miomandre, G. Clavier, M.-C. Vernières, S. Badré, R. Méallet-Renault
Laboratoire de Photophysique et
Photochimie Supramoléculaires et Macromoléculaires
UMR 8531, Ecole Normale Supérieure de Cachan
61 Av. du P[t] Wilson, 94235 Cachan (France)
Fax: (+33) 147-402-454
E-mail: audebert@ppsm.ens-cachan.fr

we compare the same features for the already known dichloro-*s*-tetrazine **1**.

Results and Discussion

Electrochemistry: We have already demonstrated that tetrazines bearing aromatic substituents are reversibly reducible into a relatively stable anion radical.[11] The aim of the electrochemical study was twofold: first, to investigate the potential ability of the anion radical of chlorotetrazines to cleave into a tetrazinyl radical and a chloride ion; and second, to check the sensitivity of the reduction potential to chemicals, especially electron-rich compounds. Indeed it had been suggested in the literature,[9] that tetrazines should be able to coordinate to fluoride ions, and hence there was a possibility that the redox potential could be affected by the addition of halide ions or electron-rich aromatic compounds.

The results of electrochemistry measurements show that all the tetrazine compounds investigated are reducible, either in acetonitrile or in dichloromethane, giving well defined, fully reversible cyclic voltammograms (CVs), as depicted on Figure 1. CVs are reversible whatever the chlorine content. Apparently the tetrazine ring is electrodeficient enough to prevent a chlorine atom to be expelled from the anion radical. The electronic exchange is quite fast, since at rather low scan rates, the peak-to-peak separation (ca. 70 mV) remains close to the theoretical value. Actually, CVs performed at scan rates higher than $1\,V s^{-1}$ display a dependence of the peak potentials with logarithm of scan rate characteristic of a quasi-reversible redox system, corresponding to a standard heterogeneous rate constant of about $10^{-2}\,cm\,s^{-1}$.

Figure 1a clearly demonstrates the influence of the substituent on the position of the redox peak. While changing an electroattracting group such as -Cl into a donating group such as $-OCH_3$ a negative shift of the reduction potential of about 280 mV is induced. The standard potentials are given in Table 1 and correlate well with the Taft–Hammett σ^- constants. Concerning the two-tetrazine moiety compound **5** (see Figure 1b), CV displays a one-step reduction process with a bielectronic exchange (peak current is quite the same as for **3**, while this latter was twice more concentrated), as expected for a substrate with two non-interacting electroactive moieties.[14] Interestingly, the diffusion coefficients in solution (Table 1) are slightly lower for tetrazine compounds than for ferrocene although the latter is larger. This demonstrate that tetrazines are more solvated, which is not unexpected given their strong electron-attracting character.

Table 1. Standard potentials, relative diffusion coefficients (vs. ferrocene) and overall Taft–Hammett coefficients for the tetrazine derivatives reduction in dichloromethane on glassy carbon electrode.

Tetrazine/Electrochemical data	**1**	**2**	**3**	**4**	**5**
E^0 (V vs Ag^+/Ag)	−0.48	−0.77	−1.02	−0.75	−0.77
D/D_{Fc}	0.55	0.62	0.56	0.55	0.73
$\Sigma\sigma^-$	−0.46	−0.68	−0.90	−0.63	−0.68

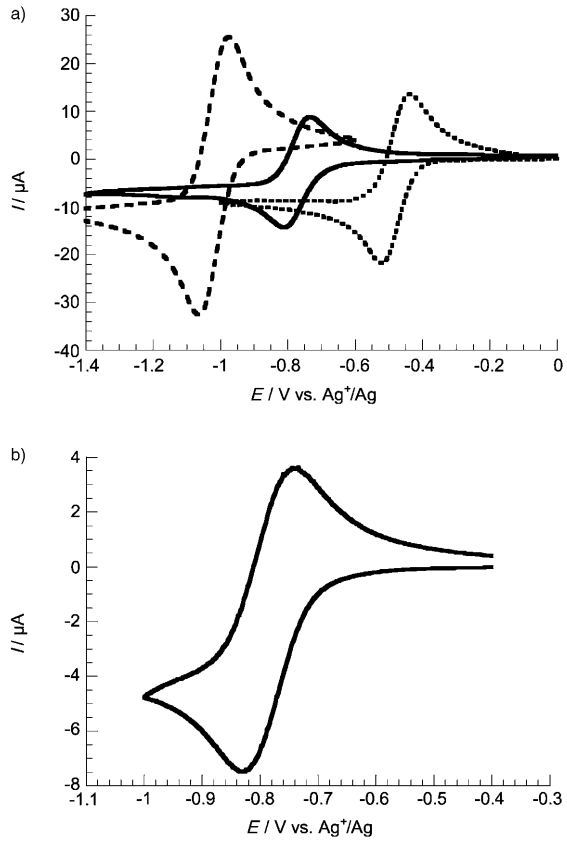

Figure 1. CV of a) **1** (-----), **2** (– – –), **3** (——); and b) **5** in dichloromethane (+ TBAP) on glassy carbon electrode at $0.1\,V s^{-1}$. CV of compound **4** is similar to **3** and was not displayed for clarity purpose. Concentrations are about 10 mM except for **5** (5 mM).

Some attempts were made to investigate the influence of halides added (all of which have been tested) and electron-rich substances (phenol, anisole and triphenylamine) on the redox potential of the tetrazine (compound **1** was chosen as the model substrate). No potential shift was observed, as it should have been the case, if the formation of a somewhat stabilized adduct between the neutral tetrazine and the electron-rich added compound had occurred. However, in the case of acidic aromatic compounds such as phenol and especially 4-nitrophenol, a positive shift of the reduction potential of the tetrazine, as well as a strong decrease of the reoxidation current has been observed (see Figure 2). These facts give evidence for an efficient proton transfer between the basic anion radical of the tetrazine compound and the phenolic moiety.

Theoretical modelling: Geometry optimisation has been completed for tetrazines **1**–**3** (see Experimental Section for details). All of the tetrazines investigated are completely planar, confirming a good electronic interaction between the cycle and its substituents. Figure 3 shows the frontier orbitals HOMO, LUMO and the two lying next to them

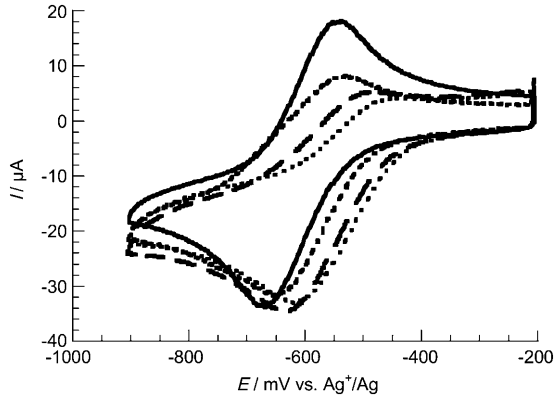

Figure 2. CVs of compound **1**, 5 mM in dichloromethane on glassy carbon at 1 $V s^{-1}$, in presence of 4-nitrophenol: 0 equiv (——), 2 equiv (-----), 5 equiv (– – –), 7 equiv (•••••).

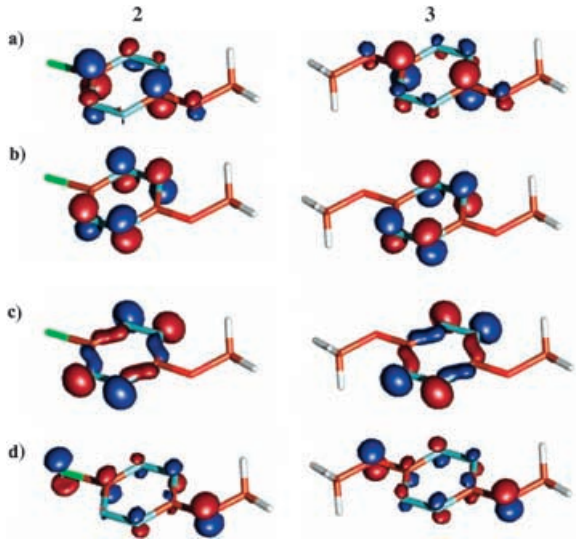

Figure 3. Plots of HOMO (c), LUMO (b) and the two next ones HOMO−1 (d) and LUMO+1 (a) for compound **2** (left column) and **3** (right column).The relative positions of these energy levels are indicated in the insert frame for compounds **1**–**3**.

HOMO−1 and LUMO+1, in the case of compounds **2** and **3**. They are antisymmetrical and symmetrical, respectively, to a plane perpendicular to the tetrazine ring and passing through the C_3 and C_6 atoms. The HOMO and LUMO electronic densities appear to be localised solely on the ring nitrogens. However, no MO coefficient is present on the substituents for the considered molecules in these orbitals, which seems to indicate that their influence on the observed electrochemical behavior of the tetrazine is mainly due to their inductive effect.

On the other hand, the configuration interaction calculation performed on these molecules were disappointing as no transition was found in the visible region. This method does not seem to be appropriate to explain the observed photophysical results (see below).

UV/Vis spectroscopy: The UV/visible spectra were recorded in dichloromethane and are shown in Figure 4. They display a very strong band in the UV region, corresponding to the π–π* allowed transition, and a much less intense band in the visible region, corresponding to the n–π* transition, which is responsible for the color of the compounds. The UV band maximum wavelength correlates clearly with the donor–acceptor balance of the substituent. When the chloro moiety is substituted by a methoxy group, a red shift of the absorption band is observed. This shift is stronger for the UV band than for the visible one. As shown by the molecular orbital diagrams, the π–π* allowed transition position is much more sensitive to substituent effects than the n–π* transition, as was previously observed.[9] The absorption maxima are listed in Table 2, along with the extinction coefficients and the fluorescence characteristics of the tetrazine compounds.

Fluorescence in solution: The fluorescence spectra of the tetrazine compounds have been recorded both in solution and in the crystalline state, in addition to their decay times (λ_{ex} = 495 nm). The fluorescence of heteroatom-substituted tetrazines has been already observed,[13] although much more data can be found on calculated spectra than on actual measurements.[15–17] It seems that fluorescence is a property of some tetrazines substituted by heteroatoms directly on the ring, because up to now no bisaryltetrazine has been found to be fluorescent.[11–12] The spectra in solution are shown in Figure 5 and indicate the spectral shape and position of the band. The fluorescence decays (Figure 6) have also been investigated and show long lifetimes (several tens of ns) with monoexponential behavior, as expected for small molecules in solution if only one population of molecules is encountered. Compound **4** shows a biexponential behavior with a very short lifetime; this might be due to the contribution of the naphthalene moiety.

For symmetric molecules **1** and **3**, lifetimes are all in the same range (50 to 60 ns) and quantum yields are close. On the contrary, the chloromethoxytetrazine **2** shows a three

Table 2. Spectroscopic features of the tetrazine derivatives (recorded in dichloromethane).

Compound	Absorption maximum wavelengths [nm]	Emission maximum wavelengths [nm]	Molar extinction coefficient of the (n–π*) transition [$cm^{-1} L mol^{-1}$]	Lifetime of the excited state [ns] (λ_{ex} = 495 nm)	Fluorescence quantum yield
1	307–515	551–567	460	58	0.14
2	269–327–520	567	1900	160	0.38
3	275–345–524	575	663	49	0.11
4	281–523	338[a] 567[b]	573	120; 6[c]	0.004[b]
5	270–328–521	572	1170	144	0.36

[a] Excitation at 281 nm. [b] Excitation at 524 nm. [c] Biexponential decay.

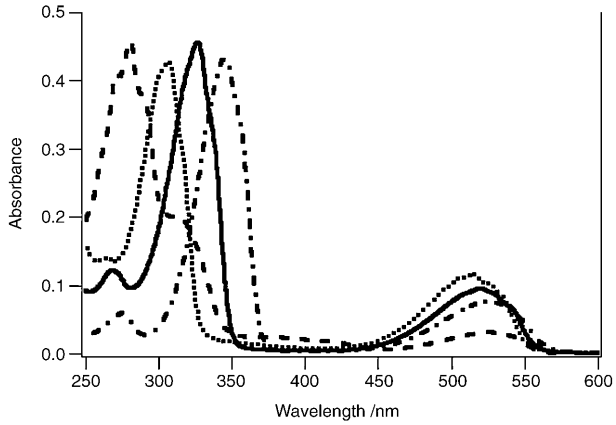

Figure 4. Absorption spectra of compounds **1** (•••••), **2** (——), **3** (-·-·-·), and **5** (– – –) in dichloromethane.

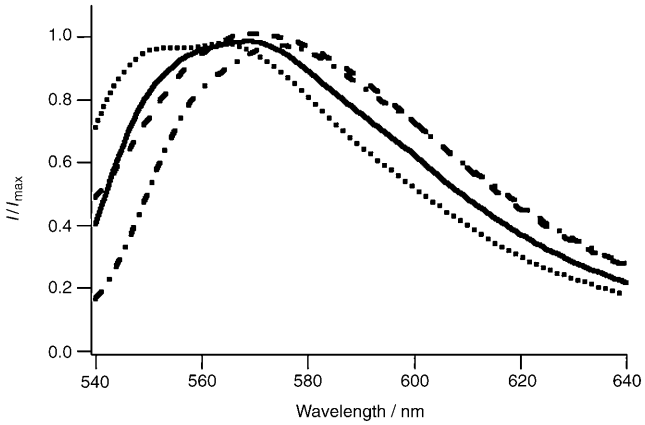

Figure 5. Fluorescence emission spectra of compounds **1** (•••••), **2** (——), **3** (-·-·-·), and **5** (– – –), in dichloromethane. Excitation wavelength is 495 nm.

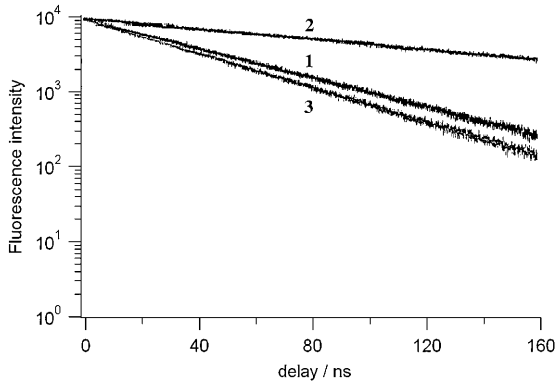

Figure 6. Fluorescence decays of compounds **1**–**3** in dichloromethane (excitation wavelength 495 nm).

times higher quantum yield and a very long lifetime. This very unusual behavior is interesting in view of potential sensor applications and will be the topic of more detailed investigations and computational analysis in the future.

Fluorescence in the solid state: Interestingly these molecules show luminescent properties in the solid state (Table 3). The less promising candidate is naphthoxytetrazine **4**. The fluorescence is weak both in CH_2Cl_2 and in the solid state. Millimeter-size crystals of the "family" of the three disubstituted tetrazines **1**-**3** and the bridged compound **5** are actually luminescent under the microscope. The spectral shift observed in CH_2Cl_2 for the three disubstituted tetrazines remains valid in the solid state when going from the chloro to the methoxy group. The spectral shape is preserved, although the band is narrowing. This might be due to less accessible deactivation processes. Indeed in CH_2Cl_2 the band broadening can be ascribed to solvent–tetrazine interactions.

Table 3. Maximum emission wavelengths and lifetimes of tetrazine compounds in the powder state (excitation wavelength at 495 nm).

Compound	Max. emission wavelength [nm]	Lifetime [ns]
1	555	17.8
2	560	19.1
3	569	16.0
4	563	0.7[a]
5	559.5	12.6[b]
		8–9[c]

[a] Multiexponential. [b] Monoexponential (excitation at the crystal centre). [c] Multiexponential (excitation at the crystal edge).

Concerning the decay times, one can see that the fluorescence lifetime is strongly decreased in the solid state compared with the solvent environment (roughly 4–5 times lower). Nevertheless, the decay times are generally monoexponential with a lifetime between 10 and 20 ns. Such a monoexponential behavior shows that only one population of fluorophores can emit light; this indicates very few interactions between molecules in the solid state. The fact that the spectrum shape is roughly preserved and fluorescent properties are not completely lost also gives evidence that only a weak intermolecular coupling occurs in the solid state.

The fluorescence decay of compound **5** shows a different behavior with a dependence on the position of the excitation relative to the crystal (Figure 7). Indeed, if the center of a single millimeter-size crystal is irradiated, the decay is monoexponential with a 12.6 ns lifetime; conversely when the excitation is focused on the crystal edge, one can observe a multiexponential decay, with an average lifetime of 8 to 9 ns. This behavior might be due to crystal surface defects, which act as quenchers for the exciton. Nevertheless, we will carry out a complete study of the solid state luminescent properties, focusing especially on the influence of the crystal size[18] and solvent evaporation.

Fluorescence quenching: In order to investigate the possible use of these molecules as sensor agents, we have studied the fluorescence quenching by electron-rich rings, of either aprotic compounds such as anisole or tertiary amines or protic compounds such as phenol or 4-nitrophenol. The tetrazine **5** was selected as potential "tweezer" for donor sub-

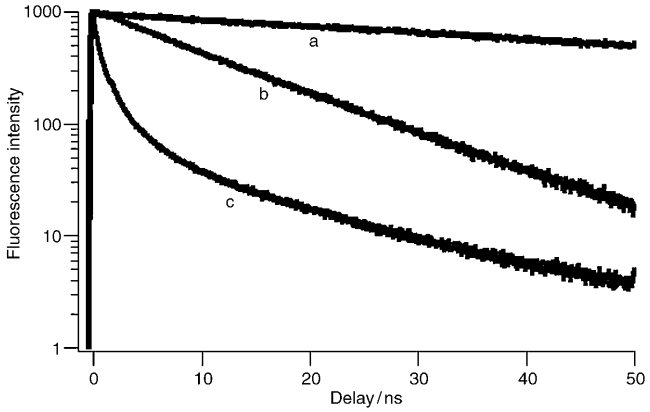

Figure 7. Fluorescence decays of compound **5**: a) reference decay in CH_2Cl_2; b) in the powder state (excitation at the centre of a millimetre-size crystal); c) in the powder state (excitation at the crystal edge).

strates, because it can possibly act as a two-sided acceptor. In all cases the electron-rich aromatic compounds have been shown to quench the fluorescence of the tetrazine excited state, in the visible range, according to the Stern–Volmer Equation:

$$\frac{I_0}{I} - 1 = k_q \cdot \tau_0 \cdot [Q]$$

where I and I_0 are the intensities in presence and absence of quencher, respectively; k_q is the quenching constant; τ_0 is the tetrazine lifetime; and $[Q]$ is the quencher concentration. This is shown in Figure 8, which depicts the Stern–

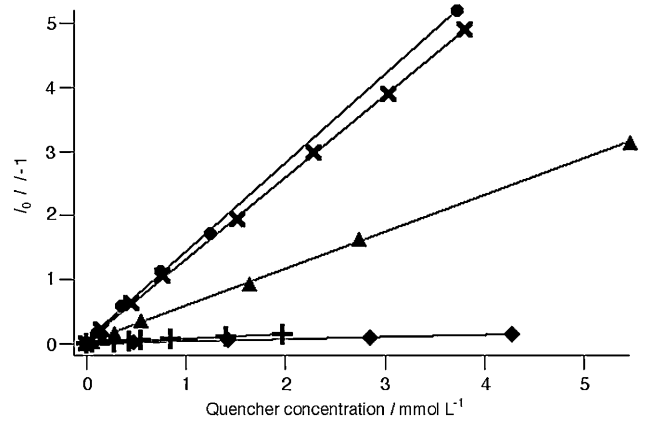

Figure 8. Stern–Volmer plots for compound **5** as functions of quencher concentrations for the various quenchers: ● triphenylamine; × tris-*p*-bromophenylamine; ▲ phenol; + 4-nitrophenol; ◆ anisole.

Volmer plots in the case of several quenchers. Table 4 summarizes the Stern–Volmer slopes ($K_{SV} = k_q \cdot \tau_0$) for the various quenchers.

The quenching mechanism can be either static or dynamic. Considering a dynamic quenching (diffusion controlled mechanism), the diffusional rate constant (k_q) calculated

Table 4. Stern–Volmer slopes K_{SV} for the fluorescence quenching of compound **5**, in presence of the indicated quenchers (from Figure 8).

Quencher	Stern–Volmer slope (K_{SV} in mol^{-1}L)
triphenylamine	1400
tri-*p*-bromophenylamine	1250
phenol	580
4-nitrophenol	80
anisole	40

from fluorescence lifetimes and Stern–Volmer slopes would range from 3.10^8 to 10^9 L mol^{-1} s^{-1}. These values are not in good agreement with usual diffusional rate constants in liquids, which are about 10^9–10^{10} L mol^{-1} s^{-1}.[19]

Hence we expect the quenching mechanism to be rather static, since quenching is observed when quencher concentration is in excess compared to tetrazine **5** (7.5×10^{-5} mol L^{-1}).[19] This is also in accordance with the "tweezer" structure of the tetrazine, which could allow "chelation" of the donor molecules.

It is clear that the slopes of the Stern–Volmer plots are related to the electron affinity of the quenchers: The better electron donors lead to the higher quenching constants. The Rehm–Weller Equation:

$$\Delta G^0 = E(D/D^+) - E(A/A^-) - E_{0-0} - \frac{e^2}{\varepsilon \cdot r}$$

where e is the electron charge, ε the dielectric constant of the solvent and r is the distance between the donor and acceptor. The Equation yields the free energy for the electron transfer between the two compounds. Usually it is impossible to get the exact value of r; thus it is assumed to be equal to the sum of the donor and acceptor radii. Therefore we have plotted the logarithm of the Stern–Volmer constant ($\log K = -\Delta G^0/RT$) versus the standard potential of various quenchers[20] (see Figure 9). Apart from phenol, a very good linear correlation is observed, which is indicative of the occurrence of an electron transfer between the tetrazine excited state and the donor, even in the case of protic donors. Hence electron transfer seems to be the most efficient way of fluorescence quenching for the tetrazine excited state. We

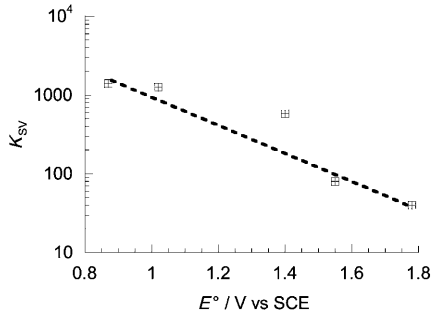

Figure 9. Correlation between the logarithm of the Stern–Volmer constant and the standard potential (vs. SCE) of the various quenchers (for symbols, see Figure 8).

can mention that similar conclusions were drawn in the case of fluorescence quenching of fluorenone by phenol derivatives, although a contribution of hydrogen-bonding interaction was proposed in the case of high oxidation potential donors.[21] In fact, further investigations are probably required in order to clearly quantify the contribution of each process (electron transfer and/or intermolecular hydrogen bonding) in the fluorescence quenching of tetrazines.

Conclusion

We have described herein the properties of several new substituted tetrazines which display a fully reversible electrochemical behavior and an intense fluorescence, both in solution and in the solid state. The fluorescence lifetimes are long (several tens of ns) and the emission can be efficiently quenched by electron donors such as aromatic compounds, which highlights the ability of these new compounds to be used in sensor devices. Work is now in progress to develop applications in that direction.

Experimental Section

Synthesis: Dichlorotetrazine **1** was obtained by the method recently described by Hiskey.[22,23] We noticed that, in the last chloration step it was important first to freshly prepare the bis(hydrazinotetrazine), and second to ensure an important flux of chlorine with a strong agitation, because of the side reactions that might occur between the starting compound and **1**. The best way was to insure a large chlorine inlet and a powerful magnetic stirrer, so that the reaction was over in 7–10 min; longer reaction times led to the formation of by-products. The reaction was finished when the solution turned clear.

CAUTION: The use of a thiosulfate filled washing funnel to quench excess chlorine outlet, as well as a ventilated hood are crucial!

The chloromethoxytetrazine **2**[24] was obtained by simple stirring of **1** in methanol at room temperature for 1 h, while dimethoxytetrazine **3**[24] was formed upon refluxing overnight in dry methanol in presence of excess dry hydrogenocarbonate. Please note that solvent dryness was important in this reaction; therefore for this latter synthesis it was also necessary to introduce a small amount of drying agent in the vessel, for example, activated molecular sieve or anhydrous magnesium sulfate to avoid substitution by adventitious water. Yield: 70–75% for **2** and 80–85% for **3**.

Compound **2**: ^{1}H NMR (300 MHz, 25°C, $CDCl_3$, TMS): $\delta = 4.34$ (OCH_3); ^{13}C NMR (300 MHz, 25°C, $CDCl_3$, TMS): $\delta = 167.1$, 164.1 (C of tetrazine), 57.5 (OCH_3); HRMS (EI): m/z: calcd for 145.9995; found: 146.0006 $[M]^+$.

Compound **3**: ^{1}H NMR (300 MHz, 25°C, $CDCl_3$, TMS): $\delta = 4.23$ (OCH_3); ^{13}C NMR (300 MHz, 25°C, $CDCl_3$, TMS): $\delta = 166.5$ (C of tetrazine), 56.7 (OCH_3); HRMS (EI): m/z: calcd for 142.0491; found: 142.0489 $[M]^+$.

Compound **4** was prepared by heating **1** (1 g) in a pressure resistant tube at 100°C with a large excess (about 10 times) of 1-naphthol in dichloromethane (5 mL) for about two hours. Yield: 54% of deep red needles. ^{1}H NMR (300 MHz, 25°C, $CDCl_3$, TMS): $\delta = 7.96$ (dd, $J = 7.54$, 2.02 Hz, 1H; H8), 7.89 (m, 2H), 7.56 (m, 2H), 7.41 (dd, $J = 7.54$, 0.92 Hz, 1H; H2); ^{13}C NMR (300 MHz, 25°C, $CDCl_3$, TMS): $\delta = 168.3$, 165.6 (C of tetrazine), 147.9 (Cq), 135.2 (Cq), 128.5 (CH), 27.5 (CH), 127.4 (CH), 127.2 (CH), 126.2 (Cq), 125.6 (CH), 120.8 (CH), 117.3 (CH); HRMS (EI): m/z: calcd for: 258.0308; found: 258.0306 $[M]^+$.

Compound **5** was prepared by heating for 3 h in a pressure resistant tube, **1** (1.4 g, 9.3 mmol), butane-1,4-diol (Aldrich Chemicals, 0.36 g, 4 mmol) in CH_2Cl_2 (2 mL) with magnesium sulphate (0.2 g) and potassium hydrogenocarbonate (0.2 g). After chromatography (CH_2Cl_2), 0.2–0.25 g of **5** were recovered (13–15%). ^{1}H NMR (300 MHz, 25°C, $CDCl_3$, TMS): $\delta =$ 3.75 (t, $J = 5.88$ Hz, 4H; OCH_2), 1.79 (t, $J = 6.31$ Hz, 4H; OCH_2CH_2); ^{13}C NMR (300 MHz, 25°C, $CDCl_3$, TMS): $\delta = 166.7$, 164.3 (C of tetrazine), 70.9 (OCH_2), 28.7 (OCH_2CH_2); MS (EI): m/z: calcd for: 318.0147; found: 318 $[M]^+$.

Electrochemistry: The electrochemical studies were performed by using an EG&G PAR 273 potentiostat, interfaced to a PC computer. Cyclic voltammetries at scan rates higher than 0.1 $V s^{-1}$ were performed by using a home made potentiostat equipped with a manual ohmic drop compensation system.[25]

The reference electrode used was an Ag^+/Ag electrode filled with 0.01 M $AgNO_3$. This reference electrode was checked vs. ferrocene as recommended by IUPAC. In our case, $E^\circ(Fc^+/Fc) = 0.118$ V in dichloromethane with 0.1 M TEAP. A platinum wire and a glassy carbon disk (1 mm diameter) were used respectively as counter and working electrodes.

Tetrabutylammonium perchlorate was purchased from Fluka (puriss.). Acetonitrile (Aldrich, 99.8%), dichloromethane (SDS, 99.9%) were used as received. All solutions were deaerated by bubbling argon gas for a few minutes prior to electrochemical measurements.

Theoretical modelling: All the geometry optimizations were performed using the hybrid density functional B3LYP potential in conjuration with a 6-31G* basis set as implemented in GAUSSIAN03W.[26] This level was adequate for the geometry optimization of aromatic compounds.[27] Harmonic vibrations were also calculated for all the obtained structures to establish that a true minimum was observed.

UV/Vis and fluorescence spectroscopy

Steady-state spectroscopy: A UV/Vis Varian CARY 500 spectrophotometer was used. Excitation and emission spectra were measured on a SPEX Fluorolog-3 (Jobin-Yvon). A right-angle configuration was used. Optical density of the samples was checked to be less than 0.1 to avoid re-absorption artifacts.

Time-resolved spectroscopy: The fluorescence decay curves were obtained with a time-correlated single-photon-counting method using a titanium/sapphire laser (82 MHz, repetition rate lowered to 4 MHz by a pulse-peaker, 1 ps pulse width, a doubling crystals was used to reach 495 nm excitation) pumped by an argon ion laser. The Levenberg–Marquardt algorithm was used for non-linear least squares fits.

The compounds were purified one additional time (obtained in the end as millimeter-size crystals), and put under a Nikon DIAPHOT 200 microscope. Fluorescence emission spectra of crystalline powders were recorded under the microscope, excitation wavelength 495 nm, by using an Ocean Optics S 2000 miniature fiber optic spectrophotometer.

[1] F. Bédioui, J. Devynck, C. Bied-Charreton, *J. Mol. Catal. A* **1996**, *92*, 1411.
[2] G. Bidan, B. Divisia-Blohorn, M. Lapkowski, J. M. Kern, J. P. Sauvage, *J. Am. Chem. Soc.* **1992**, *114*, 598.
[3] R. P. Kingsborough, T. M. Swager, *Prog. Inorg. Chem.* **1999**, *48*, whole Volume.
[4] J. P. Lang, H. Kawaguchi, K. Tatsumi, *Inorg. Chem.* **1997**, *36*, 6447.
[5] A. R. Katritzky, *Handbook of Heterocyclic Chemistry*, Pergamon Press, New York, **1986**.
[6] W. Kaim, *Coord. Chem. Rev.* **2002**, *230*, 127.
[7] M. A. El Sayed, *J. Chem. Phys.* **1963**, *38*, 2834.
[8] R. Gleiter, V. Schehlmann, J. Spanget-Larsen, H. Fischer, F. A. Neugebauer, *J. Org. Chem.* **1988**, *53*, 5756.
[9] J. Waluk, J. Spanget-Larsen, E. W. Thulstrup, *Chem. Phys.* **1995**, *200*, 201.
[10] J. Spanget-Larsen, E. W. Thulstrup, J. Waluk, *Chem. Phys.* **2000**, *254*, 135.
[11] P. Audebert, S. Sadki, F. Miomandre, G. Clavier, M. C. Vernières, M. Saoud, P. Hapiot, *New J. Chem.* **2004**, *28*, 387.

[12] P. Audebert, F. Miomandre, S. Sadki, G. Clavier, *Electrochem. Commun.* **2004**, *6*, 144.
[13] F. Gückel, A. H. Maki, F. A. Neugebauer, D. Schweitzer, H. Vogler, *Chem. Phys.* **1992**, *164*, 217.
[14] A. J. Bard, L. R. Faulkner, *Electrochemical Methods: Fundamentals and Applications*, Wiley, New York, **2002**, Chapter 12.
[15] D. H. Levy, *J. Chem. Soc. Faraday Trans. 2* **1986**, 1107.
[16] S. Ryu, R. M. Stratt, K. K. Baeck, P. M. Weber, *J. Phys. Chem. A* **2004**, *108*, 1189.
[17] C. Adamo, V. Barone, *Chem. Phys. Lett.* **2000**, *330*, 152.
[18] G. Laurent, N. T. Ha Duong, R. Méallet-Renault, R. B. Pansu, *Nanophotonics: Integrating Photochemistry, Optics, and Nano/Bio-Materials Studies*, Elsevier, Amsterdam, **2004**.
[19] B. Valeur, *Molecular Fluorescence*, Wiley-VCH, Weinheim, **2002**, Chapter 4, p. 74.
[20] Data from the *Encyclopedia of electrochemistry of the elements, Organic Section* (Eds.: A. J. Bard, H. Lund), Marcel Dekker, New York, **1978**.
[21] L. Biczok, T. Berces, H. Linschitz, *J. Am. Chem. Soc.* **1997**, *119*, 11071.
[22] D. E. Chavez, M. A. Hiskey, R. D. Gilardi, *Angew. Chem.* **2000**, *112*, 1861–1863; *Angew. Chem. Int. Ed.* **2000**, *39*, 1791–1793.
[23] D. E. Chavez, M. A. Hiskey, *J. Energ. Mater.* **1999**, *17*, 357.
[24] Z. Novak, B. Bostoi, M. Csekei, K. Lörinez, A. Kotschy, *Heterocycles* **2003**, *60*, 2653.
[25] D. Garreau, J. M. Savéant, *J. Electroanal. Chem.* **1975**, *50*, 1.
[26] Gaussian 03, Revision B.04, M. J. Frisch, G. W. Trucks, H. B. Schlegel, G. E. Scuseria, M. A. Robb, J. R. Cheeseman, J. A. Montgomery, Jr., T. Vreven, K. N. Kudin, J. C. Burant, J. M. Millam, S. S. Iyengar, J. Tomasi, V. Barone, B. Mennucci, M. Cossi, G. Scalmani, N. Rega, G. A. Petersson, H. Nakatsuji, M. Hada, M. Ehara, K. Toyota, R. Fukuda, J. Hasegawa, M. Ishida, T. Nakajima, Y. Honda, O. Kitao, H. Nakai, M. Klene, X. Li, J. E. Knox, H. P. Hratchian, J. B. Cross, C. Adamo, J. Jaramillo, R. Gomperts, R. E. Stratmann, O. Yazyev, A. J. Austin, R. Cammi, C. Pomelli, J. W. Ochterski, P. Y. Ayala, K. Morokuma, G. A. Voth, P. Salvador, J. J. Dannenberg, V. G. Zakrzewski, S. Dapprich, A. D. Daniels, M. C. Strain, O. Farkas, D. K. Malick, A. D. Rabuck, K. Raghavachari, J. B. Foresman, J. V. Ortiz, Q. Cui, A. G. Baboul, S. Clifford, J. Cioslowski, B. B. Stefanov, G. Liu, A. Liashenko, P. Piskorz, I. Komaromi, R. L. Martin, D. J. Fox, T. Keith, M. A. Al-Laham, C. Y. Peng, A. Nanayakkara, M. Challacombe, P. M. W. Gill, B. Johnson, W. Chen, M. W. Wong, C. Gonzalez, and J. A. Pople, Gaussian, Inc., Pittsburgh PA, **2003**.
[27] H. F. Bettinger, H. M. Sulzbach, P. R. v. Schleyer, H. F. Schaeffer III, *J. Org. Chem.* **1999**, *64*, 3278.

Received: December 6, 2004
Revised: April 6, 2005
Published online: July 15, 2005

